Upregulation of Glucose Metabolism During Intimal Lesion Formation Is Coupled to the Inhibition of Vascular Smooth Muscle Cell Apoptosis

Role of GSK3β

Jennifer L. Hall,[1] John C. Chatham,[2] Hagit Eldar-Finkelman,[3] and Gary H. Gibbons[1]

The purpose of this study was to define the role of metabolic regulatory genes in the pathogenesis of vascular lesions. The glucose transporter isoform, GLUT1, was significantly increased in the neointima after balloon injury. To define the role of GLUT1 in vascular biology, we established cultured vascular smooth muscle cells (VSMCs) with constitutive upregulation of GLUT1, which led to a threefold increase in glucose uptake as well as significant increases in both nonoxidative and oxidative glucose metabolism as assessed by ^{13}C–nuclear magnetic resonance spectroscopy. We hypothesized that the differential enhancement of glucose metabolism in the neointima contributed to formation of lesions by increasing the resistance of VSMCs to apoptosis. Indeed, upregulation of GLUT1 significantly inhibited apoptosis induced by serum withdrawal (control 20 ± 1% vs. GLUT1 11 ± 1%, $P < 0.0005$) as well as Fas-ligand (control 12 ± 1% vs. GLUT1 6 ± 1.0%, $P < 0.0005$). Provocatively, the enhanced glucose metabolism in GLUT1 overexpressing VSMC as well as neointimal tissue correlated with the inactivation of the proapoptotic kinase, glycogen synthase kinase 3β (GSK3β). Transient overexpression of GSK3β was sufficient to induce apoptosis (control 7 ± 1% vs. GSK3β 28 ± 2%, $P < 0.0001$). GSK3β-induced apoptosis was significantly attenuated by GLUT1 overexpression (GSK3β 29 ± 3% vs. GLUT1 + GSK3β 6 ± 1%, $n = 12$, $P < 0.001$), suggesting that the antiapoptotic effect of enhanced glucose metabolism is linked to the inactivation of GSK3β. Taken together, upregulation of glucose metabolism during intimal lesion formation promotes an antiapoptotic signaling pathway that is linked to the inactivation of GSK3β. *Diabetes* 50:1171–1179, 2001

From the [1]Division of Cardiovascular Medicine, Brigham and Women's Hospital, Harvard Medical School, Boston, Massachusetts; the [2]Department of Radiology, Division of MR Research, Johns Hopkins University School of Medicine, Baltimore, Maryland; and the [3]Department of Human Genetics, Sackler Faculty of Medicine, Tel-Aviv University, Tel-Aviv, Israel.

Address correspondence and reprint requests to Gary H. Gibbons, Cardiovascular Research Institute, Morehouse School of Medicine, 720 Westview Dr. SW, Atlanta, GA 30310-1495. E-mail: ggibbons@msm.edu.

Received for publication 8 May 2000 and accepted in revised form 11 January 2001.

DMEM, Dulbecco's modified Eagle's medium; FBS, fetal bovine serum; GFP, green fluorescent protein; GSK3β, glycogen synthase kinase 3β; NMR, nuclear magnetic resonance; PBS, phosphate-buffered solution; TCA, tricarboxylic acid; VSMC, vascular smooth muscle cell.

The risk of restenosis and atherosclerosis after balloon angioplasty is significantly elevated in individuals with diabetes (1–3). This suggests a potential link between vascular smooth muscle cell (VSMC) glucose metabolism and the progression of lesion formation. However, the contributing role of glucose metabolism to the process of vascular lesion formation in the nondiabetic population has not been defined. Recent in vivo studies from our laboratory and others indicate that intimal VSMCs seem to have an intrinsic resistance to apoptosis (4–6). We hypothesized that a component of the intrinsic property of intimal VSMCs to survive was related to a significant alteration in metabolic regulatory pathways.

VSMCs exhibit unusually high rates of glucose utilization and lactate production under normal, well-oxygenated conditions (7,8). Glucose metabolism seems to be an important determinant of vascular reactivity (9). Moreover, recent work from our laboratory has demonstrated that hyperglycemia inhibits medial VSMC apoptosis in the murine carotid artery in response to a reduction in blood flow (10). Thus, we postulated that adaptive alterations in glucose regulatory pathways and metabolism contributed to the antiapoptotic phenotype of neointimal VSMCs.

Glucose transport is the rate-limiting step in glucose metabolism and is controlled through a family of glucose transporter proteins (GLUT1–GLUT7) with GLUT1 being the predominant isoform in VSMCs (11,12). The regulation of GLUT1 in VSMCs during the formation of vascular lesions remains to be defined. Accordingly, the first aim of this study was to determine whether VSMC glucose metabolism and gene expression were altered with the progression of lesion formation.

Previous studies simulating the perturbations of glucose metabolism observed in diabetes have suggested that abnormal glucose metabolism influences vascular biology (13). Exposure to high extracellular concentrations of glucose is associated with growth of VSMCs in vitro and in vivo (13). However, the influence of alterations in glucose transporter expression on VSMC glucose metabolism and cell biology is unclear. The present study uses nuclear magnetic resonance (NMR) spectroscopy to clarify the influence of glucose transport on VSMC metabolism in the context of normal extracellular concentrations of glucose.

The cellular signaling pathways by which changes in glucose metabolism modulate VSMC biology are poorly understood. There is evidence to suggest that the induction of growth factors as well as mediators such as protein kinase C may play a role (13–15). Recent work has also suggested that glucose regulates the serine-threonine kinase, GSK3β (16). GSK3β was originally identified as one of many enzymes involved in the complex regulation of glycogen metabolism (17,18). However, GSK3β is now known to also play a critical role in protein synthesis (19), cell fate determinations (20,21), and dorsoventral axis formation in *Xenopus* (22,23). Activation of GSK3β has been shown to be proapopoptic (21). Antiapoptotic factors, including insulin, fibroblast growth factor, and epidermal growth factor, have been shown to inactivate GSK3β through phosphorylation of a serine residue at position 9 (19,24,25). Considering the multifactorial nature of GSK3β, we hypothesized that regulation of GSK3β may be a critical component linking metabolism to cell fate in the vasculature.

This is the first study to demonstrate that glucose transport and metabolism are differentially upregulated in the progression of lesion formation. Furthermore, this shift in glucose metabolism seems to be coupled to the regulation of antiapoptotic signaling pathways, in part through the inactivation of GSK3β. The notion that cellular glucose transport and metabolism are involved in orchestrating VSMC fate in the nondiabetic context is a novel concept and may have important implications for the contributing role of metabolism in vascular disease.

RESEARCH DESIGN AND METHODS

Balloon-distention injury. Male New Zealand White rabbits (2.5–4 kg) and male Sprague-Dawley rats (~300 g) were used for all experiments in accordance with protocols approved by the Standing Committee on Animals at Harvard Medical School. Animals were anesthetized with an intramuscular injection of xylazine and ketamine hydrochloride. The left common carotid artery was exposed via a 6-cm midline cervical incision. A 2-Fr Fogarty embolectomy balloon catheter was inserted retrograde through the internal carotid artery, inflated, and withdrawn to the carotid artery bifurcation as described previously (5). After a 4-week period to allow formation of a neointima, animals were killed by intravenous overdose of pentobarbital and both carotid arteries were rapidly excised. Both injured and uninjured vessels were opened en face, and the endothelial lining was gently removed before snap-freezing. In the injured vessel, the neointimal layer was gently dissected from the medial lining under a dissecting microscope and rapidly snap-frozen.

Cell culture. The clonal A7r5 rat aortic VSMCs were purchased from ATCC (Rockville, MD) and subcultured in Dulbecco's modified Eagle's medium (DMEM) with 10% fetal bovine serum (FBS; Gibco Life Technologies, Grand Island, NY) plus 1% penicillin/streptomycin (Gibco Life Technologies).

VSMCs were plated on 6-well Nunc plates in DMEM + 10% FBS for 48 h, at which time cells were near-confluent. Apoptosis was induced by serum withdrawal or treatment with Fas-ligand (100 ng/ml) (recombinant human Fas-ligand; Upstate Biotechnology, Lake Placid, NY) in the presence of 2% FBS and a mouse IgG Fas-ligand enhancer protein (Upstate Biotechnology).

Transfection strategies

Transient transfection. A7r5 VSMCs were transiently cotransfected using Lipofectamine PLUS (Gibco Life Technologies) according to the manufacturer's directions with a transfection efficiency of 15–20%. Cells were transfected with an expression vector containing the full-length GLUT1 cDNA (M. Mueckler, Washington University, St. Louis, MO) or an empty control vector, pcDNA3.1, along with the reporter gene, green fluorescent protein (GFP; Gibco Life Technologies). A subset of studies involved the transfection of an expression vector containing the full-length wild-type GSK3β cDNA (18). Transient expression of this vector results in a significant increase in GSK3β activity (18). All expression vectors were driven by cytomegalovirus promoters.

Stable transfection. Stable VSMC lines overexpressing GLUT1 were constructed using a retroviral transfection technique. A retroviral expression plasmid (pDOJ-GT1) containing the rat GLUT1 cDNA encoding the entire coding region as well as 17 and 97 bp of 5′- and 3′-nontranslated sequences (M. Birnbaum, University of Pennsylvania, Philadelphia, PA) was transiently transfected into the 293T-cell-derived Phoenix packaging cell line (G. Nolan, Stanford University, Stanford, CA) by calcium phosphate according to the manufacturer's directions (Promega, Madison, WI). A retroviral expression plasmid, pLEIN, encoding the reporter gene GFP (Clonetech, Palo Alto, CA), was similarly transfected into 293T-cells to create control transfected VSMC lines. Viral supernatant was harvested 24–72 h posttransfection, passed through a 2-μm filter, and directly applied to A7r5 VSMCs, after which G418 (500 μg/ml) was added. Upregulation of GLUT1 was confirmed by Western blotting, whereas GFP expression was tracked in living cells by fluorescent microscopy.

Western blotting. Equal amounts of protein were loaded and run on 12% polyacrylamide gels as described previously (10). Membranes were probed with various primary antibodies for the GLUT1 (L. Goodyear, Chemicon International, Temecula, CA), GLUT4 (IF8 clone; Biogenesis, Kingston, NH), total GSK3β (Quality Controlled Biochemicals, Hopkinton, MA), and ser9 phosphorylated GSK3β (Quality Controlled Biochemicals), followed by exposure to respective secondary horseradish peroxidase–linked antibodies (goat anti-rabbit, Transduction Labs, Lexington, KY; sheep anti-mouse, Amersham, Arlington Heights, IL). Membranes were treated with an enhanced chemiluminescent detection reagent and exposed to film. India ink was used to verify equal protein loading and transfer on all membranes. Computer-assisted imaging analysis was performed using Scion Image (PC version of NIH Image, Frederick, MD).

Quantitation of apoptosis. VSMC apoptosis was assessed by staining with the nuclear chromatin dye H33342 and quantitating the percentage of apoptotic nuclei in each sample (400 cells counted per sample) as described previously (10). Our laboratory has performed extensive validation of this assay in vivo and in vitro with many other techniques for assessing apoptotic cell death (5,6,10,26). The percentage of apoptotic nuclei in transiently transfected VSMC was assessed in the GFP-positive transfected subset of cells by staining with H33342 and identifying the percentage of apoptotic nuclei in the transfected population expressing GFP (75 GFP-positive cells counted per sample) as described previously (10,21).

Cell-cycle analysis. Cell-cycle analysis was assessed by fluorescence-activated cell sorter in transiently transfected GLUT1 or control transfected VSMC after a 24-h exposure to low serum–containing media (1% FBS) followed by stimulation with 10% FBS for 24 h.

Metabolic assays

Glucose uptake. Glucose uptake was quantitated with 2-[^{3}H]-deoxy-D-glucose (Du Pont–NEN, Boston, MA) as described previously (27). Briefly, cells in six-well plates were washed five times with phosphate-buffered solution (PBS), and incubated in PBS for 20 min before the addition of 1 μCi/ml radiolabeled deoxy-D-glucose. Cytochalasin B was added to a subset of wells to determine specific carrier-mediated glucose uptake. Uptake was linear between 2.5 and 10 min; thus, subsequent measurements were taken at 5 min. Uptake was immediately stopped by rinsing five times with ice-cold PBS. Cells were air-dried, solubilized in 1N NaOH, and counted in a β-counter. Data are expressed as glucose uptake in the absence of cytochalasin B minus uptake in the presence of cytochalasin B.

Glucose concentrations. Whole-tissue glucose concentrations in snap-frozen medial and neointimal specimens as well as in cell culture media (DMEM) were analyzed using an enzymatic spectrophotometric assay (HK-50; Sigma, St. Louis, MO). Glucose consumption of cultured VSMCs was calculated by subtracting the glucose concentration in the collected media from the initial glucose concentration in the media (5.5 mmol/l).

ATP content. Cellular ATP content was measured using a luciferase-based enzymatic assay from Boehringer Mannheim (Indianapolis, IN) according to the manufacturer's directions.

NMR. ^{13}C-NMR spectroscopy was used to characterize alterations in glucose metabolism as a result of stable upregulation of GLUT1 in VSMCs. The normal concentrations of glucose and pyruvate in DMEM media were replaced with 5.5 mmol/l uniformly labeled ^{13}C-glucose ([U-^{13}C]glucose) and 1 mmol/l [3-^{13}C]pyruvate. Metabolism of [U-^{13}C]glucose and [3-^{13}C]pyruvate results in the formation of [1,2-^{13}C]acetyl-CoA and [2-^{13}C]acetyl-CoA, respectively. From acetyl-CoA, the ^{13}C-label is transferred to the various tricarboxylic acid (TCA) cycle intermediates. The concentrations of the TCA cycle intermediates are below the level of detection by ^{13}C-NMR spectroscopy. However, the concentration of glutamate is high enough to be observed and is in exchange with the TCA cycle via α-ketoglutarate and aspartate aminotransferase. Thus, measurement of the ^{13}C-label incorporation into glutamate can be used as an index of entry of ^{13}C-labeled acetyl-CoA into the TCA cycle. Using the phenomenon of spin-spin coupling, it is possible to determine the relative contributions of different ^{13}C-acetyl-CoA molecules to the overall TCA cycle flux, as described

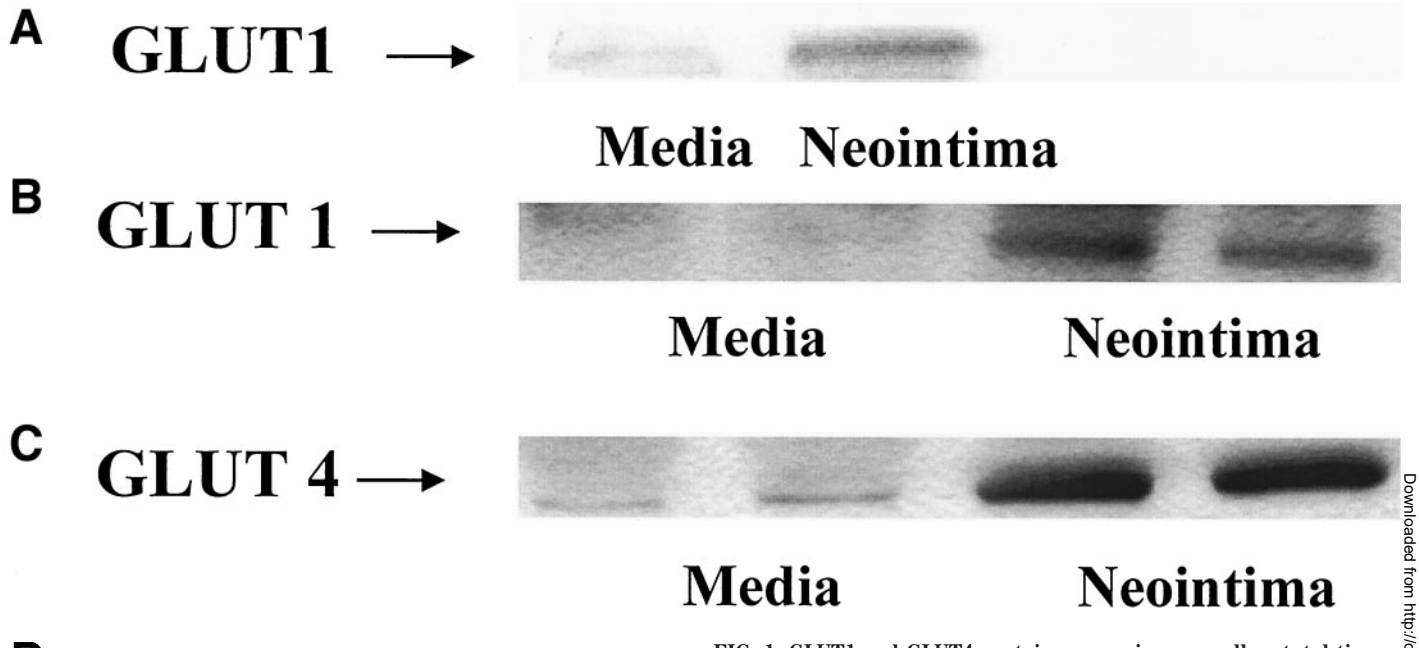

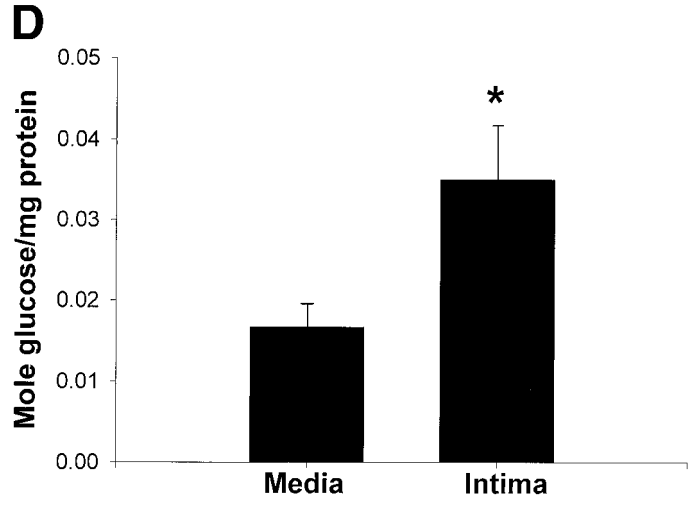

FIG. 1. GLUT1 and GLUT4 protein expression, as well as total tissue glucose content, are upregulated in isolated neointimal tissue. *A*: Representative Western blot for GLUT1 protein in rat carotid artery tissue specimens. Vessels were harvested 4 weeks after balloon injury, and the neointimal tissue was dissected away from the vessel. Representative Western blot for medial tissue was collected from an uninjured, contralateral vessel. *B*: GLUT1 protein in rabbit carotid artery tissue specimens 4 weeks after injury. *C*: GLUT4 protein in rabbit carotid artery tissue specimens 4 weeks after injury. *D*: Tissue glucose content is significantly increased in isolated neointima versus media tissue specimens. (media, 0.017 ± 0.003 mol glucose/mg protein versus neointima, 0.035 ± 0.007 mol glucose/mg protein, $n = 12$, $P < 0.01$).

in detail by Malloy et al. (28). These techniques have been used to study metabolism in intact tissues and organs as well as cells in culture (29–31). In addition to incorporation into acetyl-CoA, both glucose and pyruvate can be converted to lactate. [U-^{13}C]glucose leads to the formation of [U-^{13}C]lactate, and [3-^{13}C]pyruvate to [3-^{13}C]lactate. Thus, ^{13}C-NMR spectroscopy also allows determination of the relative contributions of exogenous glucose and pyruvate to lactate formation. ^{13}C-NMR resonances of glycogen are distinct from glucose; therefore, conversion of [U-^{13}C]glucose into glycogen can also be determined.

VSMCs with stable upregulation of GLUT1 or GFP were incubated in the labeled media for 24 h under serum-free conditions. Media were harvested and deproteinized and stored at −80°C before analysis. Cells were extracted in 6% perchloric acid (PCA) and centrifuged at 4,000*g*, and the protein-free supernatant was neutralized with KOH. The neutralized extract was stored at −80°C before analysis. Frozen superfusates were freeze-dried and resuspended in deuterium oxide, and the pH was adjusted to ~7.0.

Spectra of extracts were collected on a Bruker MSL 500-WB spectrometer (Billerica, MA) equipped with an 11.85-T magnet using a 10-mm broad-band probe as described previously (30). The relative contributions of glucose and pyruvate to acetyl-CoA entry into the TCA cycle were determined from the analysis of glutamate isotopomer distribution (30) using software developed and provided by Dr. Mark Jeffrey (TCAcalc; University of Texas Southwestern Medical Center, Dallas, TX).

Statistical analysis. Comparisons between two groups were analyzed via a Student's *t* test ($P < 0.05$), and comparisons between three or more groups were analyzed via analysis of variance with a Student-Newman-Keuls post-hoc test ($P < 0.05$). Data are presented as means ± SE.

RESULTS

Upregulation of GLUT and glucose utilization in neointimal tissue. GLUT1 protein content was significantly increased in isolated neointimal tissue compared with specimens of media tissue harvested from a balloon-injured carotid artery of a rat (Fig. 1*A*). We performed identical balloon injuries in the rabbit and detected similar increases in GLUT1 protein expression (Fig. 1*B*). Imaging analysis confirmed the significant upregulation of GLUT1 (normal uninjured vessel 638 ± 61 mean arbitrary units vs. neointima 3,546 ± 615 mean arbitrary units, $n = 4$, $P < 0.04$). In addition, GLUT4 protein expression was also significantly elevated in the rabbit neointima (Fig. 1*C*) (control uninjured vessel 1,260 ± 101 mean arbitrary units vs. neointima 5,370 ± 720 mean arbitrary units, $n = 4$, $P < 0.03$). The increase in GLUT1 and GLUT4 protein expression was accompanied by a significant elevation in total tissue glucose in neointimal tissue specimens compared with the media tissue specimens (media 0.017 ± 0.003 mol glucose/mg protein vs. neointima 0.035 ± 0.007 mol glucose/mg protein, $n = 12$, $P < 0.01$) (Fig. 1*D*). Considering the well-defined role of GLUT1 in basal-mediated glucose uptake in VSMC, we focused on the role of GLUT1 in mediating adaptive changes in VSMC remodeling.

GLUT1 upregulation significantly increases glucose uptake. We established several rat A7r5 VSMC isolates with constitutively upregulated GLUT1 expression using a retroviral expression strategy (Fig. 2*A*). In parallel, the reporter gene, GFP, was used to establish several control isolates. GLUT4 was unaltered in response to constitutive

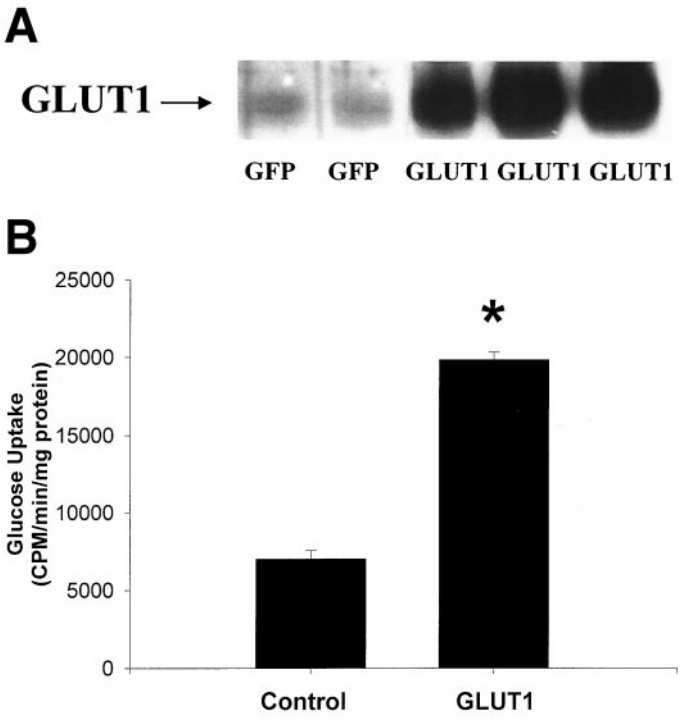

FIG. 2. GLUT1 protein expression and glucose uptake measurements in A7r5 VSMCs with constitutively upregulated GLUT1 expression. *A*: GLUT1 protein is significantly enhanced after stable transfection with a GLUT1 expression vector in several VSMC isolates. *B*: Glucose uptake, as measured with the radiolabeled glucose analog, 2-[^{3}H]-deoxy-D-glucose, is significantly elevated after constitutive upregulation of GLUT1 in cultured rat VSMCs (GFP, 7,015 ± 555 cpm · min^{-1} · mg protein^{-1} versus GLUT1, 19,844 ± 495 cpm · min^{-1} · mg protein^{-1}, n = 6, P < 0.0001). Data are expressed as means ± SE.

upregulation of GLUT1. Glucose uptake was determined with the radiolabeled glucose analog, 2-[^{3}H]-deoxy-D-glucose. Experiments were performed in the absence and presence of the fungal metabolite cytochalasin B, which inhibits facilitated glucose transport. As expected, upregulation of GLUT1 resulted in a threefold increase in facilitated glucose uptake (GFP 7,015 ± 555 cpm · min^{-1} · mg protein^{-1} vs. GLUT1 19,844 ± 495 cpm · min^{-1} · mg protein^{-1}, n = 6, P < 0.0001) (Fig. 2*B*). Glucose uptake in control transfected cells in the presence of cytochalasin B was 585 ± 123 cpm · min^{-1} · mg protein^{-1} for control transfected cells and 2,501 ± 400 cpm · min^{-1} · mg protein^{-1} for GLUT1-transfected cells, thus clearly demonstrating a specific significant increase in facilitated glucose uptake into VSMCs after GLUT1 upregulation.

We also assessed cellular glucose consumption in VSMCs with upregulated GLUT1 or GFP expression by assessing the loss of glucose in the media. Indeed, glucose consumption was significantly elevated in VSMCs with upregulated GLUT1 expression after 48 h (GFP 92.5 ± 3.2 μmol/l glucose · h^{-1} · mg^{-1} protein vs. GLUT1 115.8 ± 2.1 μmol/l glucose · h^{-1} · mg^{-1} protein, n = 6, P < 0.001). Thus, constitutive upregulation of GLUT1 in cultured VSMCs resulted in increases in intracellular glucose similar to that of neointimal tissue.

Metabolic profile of VSMC with upregulated GLUT1 expression

^{13}C-NMR spectroscopy. After glucose has entered the cell, it may enter several pathways, including glycogen synthesis, glycolysis, and the TCA cycle. Figure 3*A* shows a typical ^{13}C-NMR spectrum of a VSMC extract after incubation with [U-^{13}C]glucose and [3-^{13}C]pyruvate for 24 h.

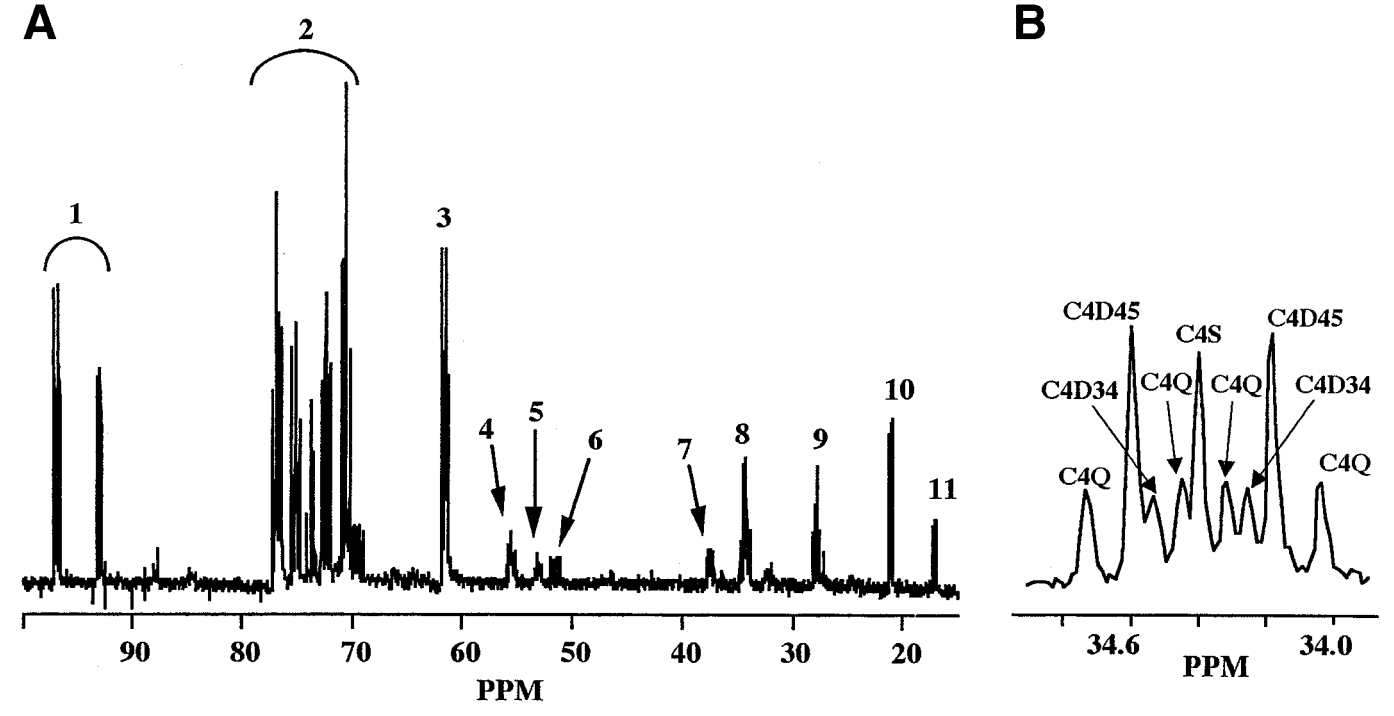

FIG. 3. *A*: High-resolution ^{13}C-NMR spectrum of a control cell extract prepared as described in RESEARCH DESIGN AND METHODS. The resonances are identified as follows: 1 = C1-glucose – α, β-anomers; 2 = C2, C3, C4, C5-glucose; 3 = C6-glucose; 4 = C2-glutamate; 5 = C2-glutamine; 6 = C2-aspartate; 7 = C3-aspartate; 8 = C4-glutamate; 9 = C3-glutamate; 10 = C3-lactate; 11 = C3-alanine. *B*: Region 8, the C4-glutamate resonances, has been expanded to demonstrate the isotopomer splitting pattern; the resonances are identified using the nomenclature as defined by Malloy et al. (28). The C4Q and C4D45 result from the metabolism of [U-^{13}C]glucose, whereas the C4D34 and C4S are from the metabolism of [3-^{13}C]pyruvate.

TABLE 1
Percent contributions of glucose, pyruvate, and unlabeled substrates to acetyl-CoA entry into the TCA cycle

	Glucose	Pyruvate	Unlabeled	Unlabeled + pyruvate
GFP	56.0 ± 1.7	28.3 ± 1.7	15.7 ± 2.6	44.0 ± 1.7
GLUT1	60.9 ± 1.0	26.1 ± 2.5	13.0 ± 1.8	39.1 ± 1.0
P	0.045	NS	NS	0.045

Data are means ± SE, $n = 4$. Metabolism of [U-^{13}C]glucose results in the formation of [1,2-^{13}C]acetyl-CoA, whereas [3-^{13}C] pyruvate will lead to [2-^{13}C]acetyl-CoA. From acetyl-CoA, the ^{13}C-label is transferred to various TCA cycle intermediates as well as to glutamate, which is in exchange with the TCA cycle. For a specific combination of unlabeled, [2-^{13}C]-, and [1,2-^{13}C]-labeled acetyl-CoA, there is a unique labeling pattern observed in the high-resolution ^{13}C-NMR spectrum. Analysis of the ^{13}C-isotopomer splitting pattern enables the calculation of the relative contributions of the different ^{13}C-labeled acetyl-CoA molecules to the TCA cycle, which directly reflects the relative contributions of the different substrates to acetyl-CoA formation. Analysis of the glutamate isotopomer distribution was performed as described in RESEARCH DESIGN AND METHODS.

Resonances from glucose, glutamate, aspartate, lactate, and alanine are all clearly evident. Incorporation of ^{13}C-label into glutamate and aspartate from transamination of the TCA cycle intermediates α-ketoglutarate and oxaloacetate, respectively, indicates the metabolism of ^{13}C-labeled glucose and pyruvate into the TCA cycle. In all of the samples, resonances from ^{13}C-glycogen were below the limit of detection. This suggests that, under the conditions of these experiments, VSMCs convert very little, if any, glucose to glycogen.

In Fig. 3*B*, the C4-glutamate resonance has been expanded to show the multiplet structure. The resonances identified as C4D45 and C4Q arise from the metabolism of [U-^{13}C]glucose and the C4D34 and C4S from metabolism of [3-^{13}C]pyruvate. Analysis of this multiplet structure, in combination with that from the C2- and C3-glutamate resonances, yields the relative contributions of glucose and pyruvate to the TCA cycle via acetyl-CoA (30).

Results from the NMR analysis are listed in Table 1. In the control transfected cells (GFP), glucose contributed 56.0 ± 1.7% acetyl-CoA entering the TCA cycle and 28.3 ± 1.7% pyruvate. Approximately 15.7 ± 2.6% acetyl-CoA originated from unlabeled substrates, presumably as a result of oxidation of amino acids present in the cell culture medium. In the GLUT1 transfected cells, there was a small but significant increase in the contribution of [U-^{13}C]glucose to acetyl-CoA entry into the TCA cycle (60.9 ± 1.0%). This was matched by a decrease in the contributions of both [3-^{13}C]pyruvate and unlabeled substrates.

From our NMR analysis, we were also able to calculate the proportion of lactate originating from glucose. There were no differences in the fraction of lactate originating from glucose in the control and GLUT1 stable transfectants (63.9 ± 1.1 vs. 65.4 ± 2.0%). However, at the end of the incubation, the ratio of [U-^{13}C]glucose to [U-^{13}C]lactate in the culture medium was significantly decreased in VSMCs with upregulated GLUT1 (GFP 6.5 ± 0.1 vs. GLUT1 5.5 ± 0.2, $P < 0.005$). A decrease in this ratio is consistent with an increase in glucose consumption and/or an increase in lactate production. These results are consistent with the increased glucose consumption we demonstrated in the VSMCs with increased GLUT1 expression.

The total protein contents of the cell extracts for the NMR studies were not significantly different between the GLUT1 and control (GFP) groups (3.7 ± 0.3 vs. 4.1 ± 0.3 mg, respectively). Therefore, the differences in the contribution of glucose to the TCA cycle and the ratio of [U-^{13}C]glucose to [U-^{13}C]lactate cannot be accounted for by differences in cell number.

ATP. To determine whether an upregulation in GLUT1 content affected cellular ATP content, we used a luciferase-based ATP assay to compare ATP content in VSMCs. Cells were exposed to growth media for 48 h followed by 24 h in serum-free media to recapitulate identical conditions for the NMR and apoptosis experiments listed above. No significant differences in cellular ATP content were found (GFP 13.8 ± 0.6 nmol/mg protein vs. GLUT1 14.0 ± 0.3 nmol/mg protein, $n = 5$, NS). Exposure of VSMCs to growth media for 72 h also had no significant effect on ATP content (GFP 13.1 ± 0.4 nmol/mg protein vs. GLUT1 12.9 ± 0.7 nmol/mg protein, $n = 5$, NS).

Enhanced glucose uptake and metabolism inhibits apoptosis and promotes growth. We were intrigued by the observation that intimal VSMCs exhibit a constitutive upregulation of GLUT1 expression in association with a resistance to apoptosis in vivo (5,6). We hypothesized that enhanced glucose uptake and metabolism are sufficient for increasing the resistance of VSMCs to apoptosis. As an initial test of this postulate, VSMCs with upregulated GLUT1 or the control transgene (GFP) were exposed to serum-free media for a period of 20 h. Constitutive upregulation of GLUT1 inhibited the percentage of VSMCs undergoing apoptosis in response to serum withdrawal (control transfected 20 ± 1% vs. GLUT1 11 ± 1%, $n = 6$, $P < 0.0005$) (Fig. 4). This antiapoptotic effect of upregulated GLUT1 expression was also demonstrated in two additional GLUT1 transfected VSMC isolates. As a further test of our hypothesis, we transiently upregulated GLUT1 and found a similar inhibition of apoptosis in response to serum withdrawal (control transfected 41 ± 3% vs. GLUT1 28 ± 2%, $n = 8$, $P < 0.002$).

Considering the local expression of the proapoptotic mediator, Fas, within neointimal lesions (32–34), we also tested whether the constitutive upregulation of GLUT1

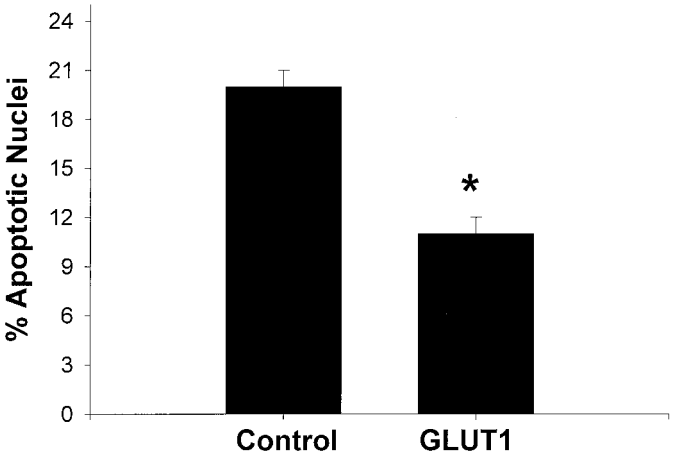

FIG. 4. Upregulation of GLUT1 significantly inhibits apoptosis induced by serum withdrawal (control transfected [GFP] 20 ± 1% vs. GLUT1 11 ± 1%, $n = 6$, $P < 0.0005$). The percentage of apoptotic nuclei was assessed 20 h after serum withdrawal by staining with H33342. Data are expressed as means ± SE.

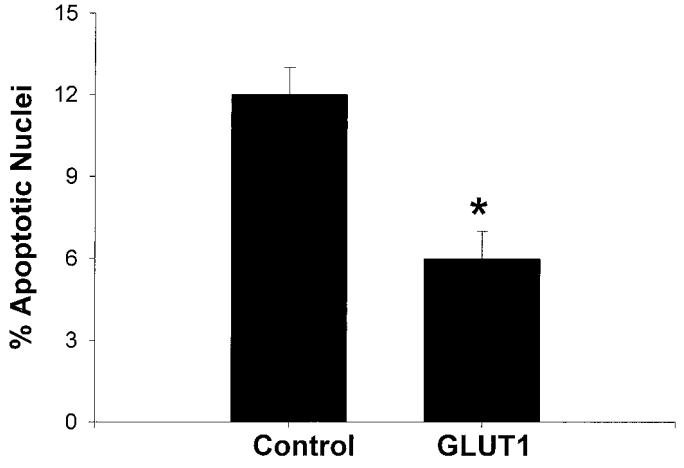

FIG. 5. Upregulation of GLUT1 significantly inhibits apoptosis induced by Fas-ligand (control transfected [GFP] + Fas-ligand, 12 ± 1% vs. GLUT1 + Fas-ligand 6 ± 1.0%, $n = 8$, $P < 0.0005$). The percentage of apoptotic nuclei was assessed 20 h after treatment by staining with H33342. Data are expressed as means ± SE.

was protective against this proapoptotic stimulus. VSMCs were assessed for apoptosis 20 h after treatment with Fas-ligand (100 ng/ml) in low serum in the presence of a Fas-ligand enhancer protein (mouse IgG). Consistent with the serum-withdrawal data, constitutive upregulation of GLUT1 also inhibited apoptosis in response to Fas-ligand (control [GFP] + Fas-ligand 12 ± 1% vs. GLUT1 + Fas-ligand 6 ± 1.0%, $n = 8$, $P < 0.0005$) (Fig. 5). These data suggest that upregulated glucose transport and metabolism protects VSMCs from apoptosis, thereby potentiating lesion formation.

To address the role of GLUT1 upregulation on VSMC growth, we performed cell-cycle analysis. Indeed, upregulation of GLUT1 resulted in a significant increase in the percentage of cells in S, G2, and M phases of the cell cycle (GLUT1 43 ± 6% vs. control [GFP] 22 ± 1%, $n = 3$, $P < 0.022$) (Fig. 6).

Differential regulation of GSK3β. Catalytically active

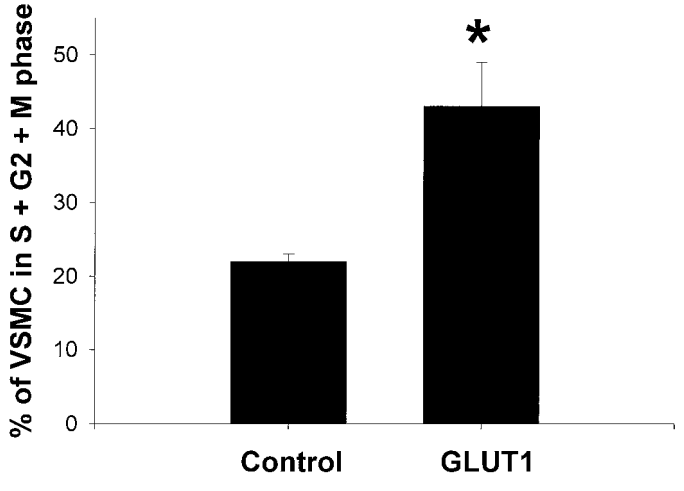

FIG. 6. Upregulation of GLUT1 results in a significant increase in entry into the cell cycle. VSMCs transiently upregulated with GLUT1 or a control vector (GFP) were exposed to low serum–containing media for 24 h, followed by stimulation with 10% FBS for 24 h. GLUT1 upregulation resulted in a significant increase in the percentage of cells in the S, G2, and M phases of the cell cycle. Data are presented as means ± SE.

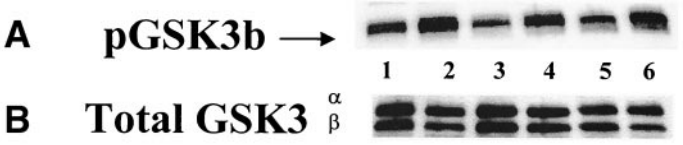

FIG. 7. *A*: Representative Western blot demonstrating enhanced phosphorylated (ser9) GSK3β protein expression in neointima (*lanes 2*, *4*, and *6*) versus isolated media (*lanes 1*, *3*, and *5*). *B*: Total GSK3β protein expression was unchanged between neointima and media.

GSK3β phosphorylates glycogen synthase and inhibits glycogen storage (18). Recent work has also demonstrated that catalytically active GSK3β induces apoptosis (21). Considering the dual function of this enzyme, we hypothesized that it may be playing a role as a critical mediator linking a nutrient signal to the fate of VSMCs. To test this postulate, we compared total and phosphorylated (ser9) GSK3β protein expression in neointimal versus medial tissue specimens. As seen in Fig. 7*A*, phosphorylation of GSK3β on ser9 was significantly enhanced in neointimal tissue, whereas total GSK3β expression was unchanged (Fig. 7*B*).

To determine whether the increased phosphorylation of GSK3β in the neointima was driven by alterations in the metabolic profile of these cells, we assessed GSK3β phosphorylation in our GLUT1 overexpressing VSMCs. Indeed, the phosphorylated form of GSK3β was significantly increased in GLUT1 overexpressing cells under fully supplemented conditions (Fig. 8*A*) as well as after 6 h of serum withdrawal (Fig. 8*B*). Total GSK3β protein expression was unchanged. This suggested that the enhanced phosphorylation state of GSK3β in the neointima was, in part, a consequence of the enhanced glucose metabolism in these cells. These findings are consistent with the working hypothesis that enhanced glucose metabolism promotes VSMC viability by inactivating the proapoptotic kinase GSK3β.

To elucidate the regulation of GSK3β as a determinant of VSMC fate, we simulated GSK3β activation by transiently upregulating the catalytically active form of GSK3β and assessing the effect on VSMC apoptosis. Indeed, upregulation of GSK3β was sufficient to induce apoptosis in VSMC (Fig. 9) (control 7 ± 1% vs. GSK3β 28 ± 2%, $n = 12$, $P < 0.0001$). To test our postulate that enhanced glucose transport and metabolism inhibited VSMC apoptosis through the inactivation of GSK3β, we transiently cotransfected GSK3β along with GFP in control previously untransfected cells and cells with stable upregulation of GLUT1. In accord with our postulate, VSMCs with constitutively upregulated GLUT1 expression were less suscep-

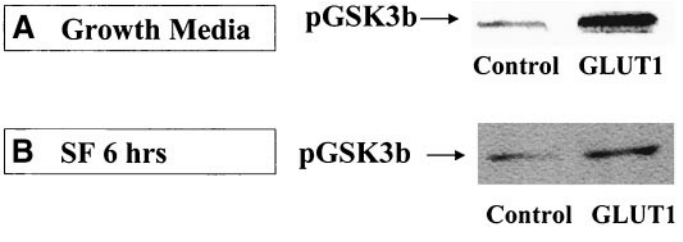

FIG. 8. Representative Western blots demonstrating enhanced phosphorylated GSK3β protein expression in A7r5 VSMCs with constitutive upregulation of GLUT1 or the control transgene (GFP) under fully supplemented conditions (*A*) as well as after 6 h of serum withdrawal (*B*).

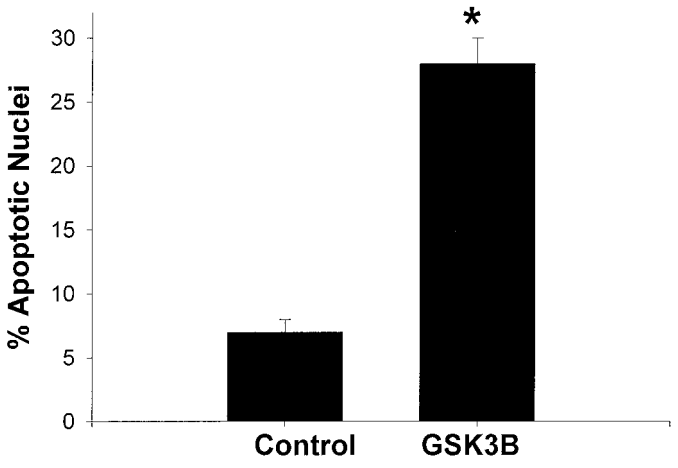

FIG. 9. Transient upregulation of catalytically active GSK3β induces apoptosis in A7r5 VSMCs. The percentage of apoptotic nuclei was assessed 20 h after serum withdrawal by staining with H33342 (control transfected 7 ± 1% vs. catalytically active GSK3β 28 ± 2%, $n = 12$, $P < 0.0001$). Data are expressed as means ± SE.

tible to GSK3β-induced apoptosis compared with control VSMCs (control 29 ± 3% vs. GLUT1 6 ± 1%, $n = 12$, $P < 0.001$) (Fig. 10). Moreover, GSK3β-mediated apoptosis was also inhibited in VSMCs with transient upregulation of GLUT1 (GLUT1 6 ± 2%, $n = 6$, $P < 0.001$). Taken together, these experiments indicate that enhanced glucose transport stimulates the phosphorylation and inactivation of the proapoptotic mediator GSK3β, in association with enhanced VSMC survival.

DISCUSSION

We have demonstrated that GLUT1 protein and intracellular glucose are differentially elevated in neointimal VSMCs compared with medial VSMCs after balloon injury. To understand the link between metabolic signaling and lesion formation, we created cultured VSMCs with constitutive upregulation of GLUT1. Upregulation of GLUT1 resulted in increases in both nonoxidative and oxidative glucose metabolism, as assessed by ^{13}C-NMR spectroscopy. This enhanced glucose transport and utilization was sufficient to inhibit apoptosis induced by serum withdrawal as well as Fas-ligand. The inhibition of apoptosis in response to two mechanistically distinct proapoptotic stimuli suggests a fundamental effect on the final common pathways regulating cell death. The coordinate increase in cell proliferation and decrease in VSMC apoptosis provides a mechanism by which enhanced glucose transport and metabolism may promote vascular lesion formation.

Coincident with the upregulation in GLUT1 expression in neointimal tissue and cultured VSMC was a significant increase in the phosphorylation state and, hence, inactivation of the proapoptotic mediator GSK3β. Transient expression of *active* GSK3β was sufficient to induce apoptosis in VSMCs. However, GSK3β-induced apoptosis was significantly attenuated by upregulation of GLUT1. Thus, our data suggest that an elevation in GLUT1 concordant with increased glucose uptake and metabolism activates an antiapoptotic signaling pathway that seems to be linked to the phosphorylation and inactivation of GSK3β in the vasculature.

This is the first study to demonstrate differential regulation of metabolic gene expression in neointimal VSMCs versus medial VSMCs after balloon injury. After vascular injury, a subset of medial VSMCs migrates into the lumen and is phenotypically modified from a contractile, differentiated state to a synthetic, "de-differentiated" phenotype (35–37). Considering that the risk of restenosis and atherosclerosis after balloon angioplasty is significantly elevated in diabetic individuals (1–3), we postulated that a component of the phenotypic modulation involved altered metabolic signaling pathways. Indeed, we found an upregulation in glucose transport, resulting in significant increases in intracellular glucose in the neointimal population. It is noteworthy that neoplastic transformation is often associated with a similar upregulation of glucose transporters (38).

We demonstrated a threefold increase in VSMC glucose uptake as a result of upregulating GLUT1. This significant upregulation of glucose transport is similar to findings in other cell systems in which GLUT1 has been upregulated, including proximal tubule-like cells, skeletal muscle, and the heart (39–41). To characterize the flux of glucose in VSMCs with upregulated GLUT1 content, we used ^{13}C-NMR spectroscopy. Upregulated glucose transport resulted in significant increases in the contribution of glucose to lactate (nonoxidative) and acetyl-CoA formation (oxidative). In contrast, glucose incorporation to glycogen was unchanged. To our knowledge, this is the first study to examine the effect of increased glucose transport on flux through both nonoxidative and oxidative pathways in VSMCs.

Studies from our laboratory and others have suggested that neointimal VSMCs are more resistant to apoptosis compared with medial VSMCs (4–6). We hypothesized that the differential upregulation of glucose transport and metabolism in neointimal VSMCs was a sufficient driving force to enhance survival of this VSMC population. Indeed, this study demonstrates that the upregulation of glucose transport significantly inhibits the percentage of VSMCs undergoing apoptosis in response to both serum with-

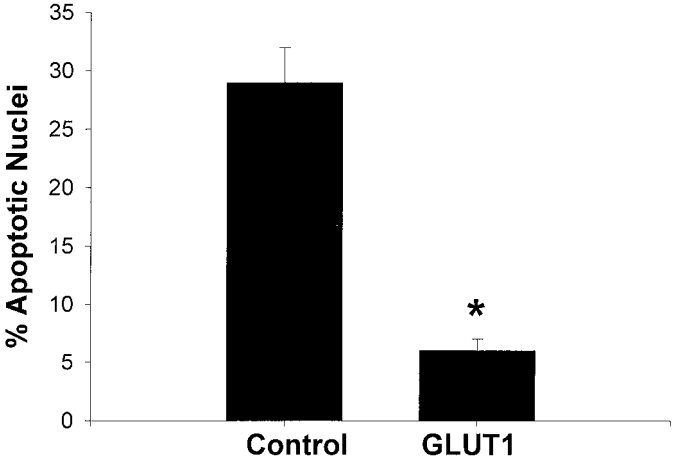

FIG. 10. Constitutive upregulation of GLUT1 inhibits GSK3β-induced VSMC death. The percentage of apoptotic nuclei was assessed 24 h after transient transfection of catalytically active GSK3β by staining with H33342 and determining the percentage of apoptotic nuclei in the transfected subset (GFP-positive). Controls were A7r5 VSMC transiently cotransfected with a control vector + GSK3β (control 29 ± 3% vs. GLUT1 6 ± 2%, $n = 6$, $P < 0.001$). Data are expressed as means ± SE.

drawal and Fas-ligand. Our findings support previous work from our laboratory and others in VSMCs, proximal tubule-like cells, and the myocardium, demonstrating that glucose metabolism is of critical importance for cell survival (10,41–43).

To our knowledge, this is the first study to demonstrate a regulatory role for GSK3β as a critical mechanistic mediator linking nutrient signaling pathways and cell fate. Moreover, the description of alterations in GSK3β phosphorylation in the vasculature has not been described previously. The enhanced phosphorylation of GSK3β in the isolated neointima is intriguing. Given the observation that GSK3β was also significantly enhanced in VSMCs stably transfected with GLUT1 suggests that the regulation of GSK3β in neointimal VSMCs may be mediated, in part, by the altered metabolic profile of these cells. A recent finding demonstrating inactivation of GSK3β by elevated glucose concentrations in rat hepatocytes lends support to our findings (16). Clearly, growth factors such as insulin, IGF-I, fibroblast growth factor, and epidermal growth factor may also be involved in the regulation. The mechanism linking increases in glucose metabolism with the inactivation of GSK3β is currently unknown. Future lines of investigation will be needed to define the regulation of GSK3β activity by glucose metabolism and the role of GSK3β as a determinant of fate in VSMCs.

It is noteworthy that the significant alterations in the regulation of GSK3β activity were not associated with detectable alterations in either glycogen content in isolated neointimal versus medial samples or cultured VSMCs. This is not surprising, considering the complex enzymatic signaling cascade involved in glycogen regulation. The role of vascular glycogen stores and its regulation remains a poorly characterized area of vascular biology. Our findings that GSK3β induces apoptosis supports and extends earlier work in nonvascular cells (21), demonstrating that the proapoptotic influence of GSK3β is contextual and determined by growth factors and glucose metabolism.

In summary, we have found that glucose transport and metabolism are differentially upregulated in the process of intimal lesion formation. Moreover, we have provided evidence to support a role for GSK3β regulation as a novel mechanistic link between upregulated glucose metabolism and an antiapoptotic cellular signaling pathway in VSMCs. These findings may have important implications for understanding the contributing role of metabolism in the process of occlusive macrovascular disease and may begin to help us understand the mechanisms underlying the elevated risk of restenosis and atherosclerosis in the diabetic population.

ACKNOWLEDGMENTS

This study was supported by grants from the National Institutes of Health (J.L.H., G.H.G., J.C.C.), the American Heart Association (J.L.H., G.H.G.), and the PEW Foundation (G.H.G.).

We thank Drs. M. Birnbaum and M. Mueckler for the GLUT1 expression constructs, Dr. L. Goodyear for the GLUT1 antibody, John Daley for his help and expertise with the fluorescence-activated cell sorter analysis, and Dr. B. Kahn for her insightful discussions.

REFERENCES

1. Brand FN, Abbott RD, Kannel WB: Diabetes, intermittent claudication, and risk of cardiovascular events: the Framingham Study. *Diabetes* 38:504–509, 1989
2. Aronson D, Rayfield EJ, Chesebro JH: Mechanisms determining course and outcome of diabetic patients who have had acute myocardial infarction. *Ann Intern Med* 126:296–306, 1997
3. Kornowski R, Mintz GS, Kent KM, Richard AD, Satler LF, Bucher TA, Hong MK, Popma JJ, Leon MB: Increased restenosis in diabetes mellitus after coronary interventions is due to an exaggerated intimal hyperplasia: a serial intravascular ultrasound study. *Circulation* 95:1366–1369, 1997
4. Bauriedel G, Shluckebier S, Hutter R, Kankdolf R, Luderitz B, Prescot MF: Apoptosis in restenosis versus stable angina atherosclerosis. *Arterioscler Thromb Vasc Biol* 18:1132–1139, 1998
5. Pollman MJ, Hall JL, Gibbons GH: Determinants of vascular smooth muscle apoptosis after balloon angioplasty: influence of redox state and cell phenotype. *Circ Res* 84:113–121, 1999
6. Pollman MJ, Hall JH, Mann MJ, Zhang L, Gibbons GH: Inhibition of neointimal cell Bcl-x expression induces apoptosis and regression of vascular disease. *Nature Med* 4:222–227, 1998
7. Campbell JD, Paul RJ: The nature of fuel provision for the Na^+-K^+-ATPase in vascular smooth muscle. *J Physiol (Lond)* 447:67–82, 1992
8. Hardin CD, Raeymaekers L, Paul RJ: Comparison of endogenous and exogenous sources of ATP in fueling Ca^{2+} uptake in smooth muscle plasma membrane vesicles. *J Gen Physiol* 99:21–40, 1992
9. Lund DD, Faraci FM, Miller FJ Jr, Heistad DD: Gene transfer of endothelial nitric oxide synthase improves relaxation of carotid arteries from diabetic rats. *Circulation* 101:1027–1033, 2000
10. Hall JL, Matter C, Pollman MJ, Bai HZ, Inishi Y, Gibbons GH: Hyperglycemia inhibits vascular smooth muscle cell apoptosis through a protein kinase C-dependent pathway. *Circulation* 98:574–580, 2000
11. Rumble JR, Cooper ME, Soulis T, Wu L, Yousself S, Gilbert RE: Vascular hypertrophy in experimental diabetes: role of advanced glycation end products. *J Clin Invest* 99:1016–1027, 1997
12. Klip A, Tsakiridis T, Marette A, Oritz P: Regulation of expression of glucose transporter by glucose: a review of studies in vivo and in cell culture. *FASEB J* 8:43–53, 1994
13. Koya D, King GL: Protein kinase C activation and the development of diabetic complications. *Diabetes* 47:859–866, 1998
14. Natarajan R, Bai W, Lanting L, Gonzales N, Nadler J: Effects of high glucose on vascular endothelial growth factor expression in vascular smooth muscle cells. *Am J Physiol Heart Circ Physiol* 273:H2224–H2231, 1997
15. Yerneni KK, Bai W, Khan BV, Medford RM, Natarajan R: Hyperglycemia-induced activation of nuclear transcription factor κB in vascular smooth muscle cells. *Diabetes* 48:855–864, 1999
16. Auer KL, Contessa J, Brenz-Verca S, Pirola L, Rusconi S, Cooper G, Abo A, Wymann MP, Davis RJ, Birrer M, Dent P: The Ras/Rac1/Cdc42/SEK/JNK/c-Jun cascade is a key pathway by which agonists stimulate DNA synthesis in primary cultures of rat hepatocytes. *Mol Biol Cell* 9:561–573, 1998
17. Parker PJ, Caudwell FB, Cohen P: Glycogen synthase from rabbit skeletal muscle: effect of insulin on the state of phosphorylation of the seven phosphoserine residues in vivo. *Eur J Biochem* 103:227–234, 1983
18. Eldar-Finkelman H, Argast GM, Foord O, Fischer EH, Krebs EG: Expression and characterization of glycogen synthase kinase-3 mutants and their effect on glycogen synthase activity in intact cells. *Proc Natl Acad Sci U S A* 93:10228–10233, 1996
19. Welsh GI, Proud CG: Glycogen synthase kinase-3 is rapidly inactivated in response to insulin and phosphorylates eukaryotic initiation factor eIF-2B. *Biochem J* 294:625–629, 1993
20. Siegfried E, Chou TB, Perrimon N: Wingless signaling acts through zeste-white 3, the Drosophila homolog of glycogen synthase kinase-3, to regulate engrailed and establish cell fate. *Cell* 71:1167–1179, 1992
21. Pap M, Cooper GM: Role of glycogen synthase kinase-3 in the phosphatidylinositol 3-kinase/Akt cell survival pathway. *J Biol Chem* 273:19929–19932, 1998
22. He X, Saint-Jeannet JP, Woodgett JR, Varmus HE, Dawid IB: Glycogen synthase kinase-3 and dorsoventral patterning in Xenopus embryos. *Nature* l374:617–622, 1995
23. Yost C, Farr GH, Pierce SB, Ferkey DM, Chen MM, Kimelman D: GBP, an inhibitor of GSK-3, is implicated in Xenopus development and oncogenesis. *Cell* 93:1031–1041, 1998
24. Summers SA, Kao AW, Kohn AD, Backus GS, Roth RA, Pessin JE, Birnbaum MJ: The role of glycogen synthase kinase 3beta in insulin-stimulated glucose metabolism. *J Biol Chem* 274:17934–17940, 1999
25. Cross DA, Alessi DR, Cohen P, Andjelkovich M, Hemmings BA: Inhibition

of glycogen synthase kinase-3 by insulin is mediated by protein kinase B. *Nature* 378:785–789, 1995
26. Pollman MJ, Yamada T, Horiuchi M, Gibbons GH: Vasoactive substances regulate vascular smooth muscle cell apoptosis: countervailing influences of nitric oxide and angiotensin II. *Circ Res* 79:748–756, 1996
27. Shepard PR, Gnudi L, Tozzo E, Yang H, Leach F, Kahn BB: Adipose cell hyperplasia and enhanced glucose disposal in transgenic mice overexpressing GLUT4. *J Biol Chem* 268:22243–22246, 1993
28. Malloy CR, Sherry AD, Jeffrey FMH: Analysis of tricarboxylic acid cycle of the heart using 13C isotope isomers. *Am J Physiol Endocrinol Metab* 259:H987–H995, 1990
29. Allen TM, Hardin CD: Pattern of substrate utilization in vascular smooth muscle using 13C isotopomer analysis of glutamate. *Am J Physiol Heart Circ Physiol* 275:H2227–H2235, 1998
30. Chatham JC, Gao Z-P, Forder JR: The impact of 1 week of diabetes on the regulation of myocardial carbohydrate and fatty acid oxidation. *Am J Physiol Endocrinol Metab* 277:E342–E351, 1999
31. Bouzier AK, Goodwin R, de Gannes FM, Valeins H, Voisin P, Canoni P, Merle M: Compartmentation of lactate and glucose metabolism in C6 glioma cells: a 13C and 1H NMR study. *J Biol Chem* 273:27162–27169, 1998
32. Bennett M, Macdonald K, Chan S, Luzio JP, Simari R, Weissberg P: Cell surface trafficking of Fas: a rapid mechanism of p53-mediated apoptosis. *Science* 282:290–293, 1998
33. Fukuo K, Nakahashi T, Nomura S, Hata S, Suhara T, Shimizu M, Tamatani M, Morimoto S, Kitamura Y, Ogihara T: Possible participation of Fas-mediated apoptosis in the mechanism of atherosclerosis. *Gerontology* 43 (Suppl. 1):35–42, 1997
34. Geng YJ, Henderson LE, Levesque EB, Muszynski M, Libby P: Fas is expressed in human atherosclerotic intima and promotes apoptosis of cytokine-primed human vascular smooth muscle cells. *Arterioscler Thromb Vasc Biol* 10:2200–2208, 1997
35. Thyberg J: Phenotypic modulation of smooth muscle cells during formation of neointimal thickenings following vascular injury. *Histol Histopathol* 13:81–91, 1998
36. Aikawa M, Sakomura Y, Ueda M, Kimura K, Manabe I, Ishiwata S, Komiyama N, Yamagucki H, Yazaki Y, Nagai R: Redifferentiation of smooth muscle cells after coronary angioplasty determined via myosin heavy chain expression. *Circulation* 96:82–90, 1997
37. Majesky MW, Giachelli CM, Reidy MA, Schwartz SM: Rat carotid neointimal smooth muscle cells reexpress a developmentally regulated mRNA phenotype during repair of arterial injury. *Circ Res* 71:759–768, 1992
38. Glick RP, Unterman TG, Lacson R: Identification of insulin-like growth factor (IGF) and glucose transporter-1 and –3 mRNA in CNS tumors. *Regul Pept* 48:251–256, 1993
39. Heilig CW, Concepcion L, Riser BL, Freytag SO, Zhu M, Cortes P: Overexpression of glucose transporters in rat mesangial cells cultured in a normal glucose milieu mimics the diabetic phenotype. *J Clin Invest* 96:1802–1814, 1995
40. Gulve EA, Ren J, Marshall BA, Gao J, Hansen PA, Holloszy JO, Mueckler M: Glucose transport activity in skeletal muscles from transgenic mice overexpressing GLUT1. *J Biol Chem* 269:18366–18370, 1994
41. Malhotra R, Brosius FC 3rd: Glucose uptake and glycolysis reduce hypoxia-induced apoptosis in cultured neonatal rat cardiac myocytes. *J Biol Chem* 274:12567–12575, 1999
42. Dominguez JH, Song B, Liu-Chen S, Qulali M, Howard R, Lee C, McAteer J: Studies of renal injury II: activation of the glucose transporter 1 (GLUT1) gene and glycolysis in LLC-PK1 cells under calcium stress. *J Clin Invest* 98:395–404, 1996
43. Schaffer SW, Croft CB, Solodushko V: Cardioprotective effect of hyperglycemia: effect on hypoxia-induced apoptosis and necrosis. *Am J Physiol Heart Circ Physiol* 278:H1948–H1954, 2000